Structural and functional analysis of the middle segment of hsp90: implications for ATP hydrolysis and client protein and cochaperone interactions

Article (Published Version)

Molecular Cell, Vol. 11, 647–658, March, 2003, Copyright ©2003 by Cell Press

Structural and Functional Analysis of the Middle Segment of Hsp90: Implications for ATP Hydrolysis and Client Protein and Cochaperone Interactions

Philippe Meyer,[1] Chrisostomos Prodromou,[1] Bin Hu,[2] Cara Vaughan,[1] S. Mark Roe,[1] Barry Panaretou,[2] Peter W. Piper,[3] and Laurence H. Pearl[1,*]

[1]Section of Structural Biology
The Institute of Cancer Research
Chester Beatty Laboratories
237 Fulham Road
London SW3 6JB

[2]Division of Life Sciences
King's College London
Franklin-Wilkins Building
150 Stamford Street
London SE1 9NN

[3]Department of Biochemistry and Molecular Biology
University College London
Gower Street
London WC1E 6BT
United Kingdom

Summary

Activation of client proteins by the Hsp90 molecular chaperone is dependent on binding and hydrolysis of ATP, which drives a molecular clamp via transient dimerization of the N-terminal domains. The crystal structure of the middle segment of yeast Hsp90 reveals considerable evolutionary divergence from the equivalent regions of other GHKL protein family members such as MutL and GyrB, including an additional domain of new fold. Using the known structure of the N-terminal nucleotide binding domain, a model for the Hsp90 dimer has been constructed. From this structure, residues implicated in the ATPase-coupled conformational cycle and in interactions with client proteins and the activating cochaperone Aha1 have been identified, and their roles functionally characterized in vitro and in vivo.

Introduction

Hsp90 plays a key role in facilitating the activity of "client" proteins involved in regulatory and signaling systems in eukaryotic cells (reviewed in Pearl and Prodromou, 2002). Hsp90s chaperone activity depends on binding and hydrolysis of ATP (Panaretou et al., 1998; Obermann et al., 1998; Grenert et al., 1999), coupled to a conformational cycle, involving opening and closing of a dimeric "molecular clamp" via transient association of the N-terminal domains (Prodromou et al., 2000; Chadli et al., 2000). ATP binds to the N-terminal domain of Hsp90 (Prodromou et al., 1997a; Grenert et al., 1997), which also binds the antitumor antibiotics geldanamycin and radicicol (Stebbins et al., 1997; Roe et al., 1999) that inhibit ATPase activity and disrupt client protein activation in vivo (Chavany et al., 1996; Schulte et al., 1995; Whitesell et al., 1994). Despite progress in understanding the mechanistic biochemistry of Hsp90 itself, little is known about how the ATPase-coupled conformational chaperone cycle promotes client protein activation, or even where and how Hsp90 interacts with its disparate, but nonetheless specific, clients.

Previous in vitro studies had suggested client protein binding sites in N-terminal and C-terminal domains of Hsp90, (Young et al., 1997; Scheibel et al., 1998); however, these utilized peptides and denatured proteins not known to be Hsp90 clients in vivo. Furthermore, Hsp90 in vivo is not involved in binding of denatured proteins (Nathan et al., 1997), so the significance of these studies is unclear. More recently, the middle segment of Hsp90 was identified as the binding site for the protein kinase PKB/Akt (Sato et al., 2000), identified as an authentic Hsp90 client by downregulation in cells treated with geldanamycin derivatives (Clarke et al., 2000).

The conformational flexibility of intact eukaryotic Hsp90 presents considerable difficulties for crystallography, and although crystals have been described (Prodromou et al., 1996), no structure has yet been reported. We utilized limited proteolysis to identify functional domains (Figure 1A) that are more amenable to structural studies, and have now determined the crystal structure of the middle 33 kDa segment of yeast Hsp90 (residues 273–560). The structure confirms the architectural similarity to other dimeric GHKL protein family members such as MutL and GyrB, but reveals considerable evolutionary divergence, including an additional domain with a new fold, and an unusual amphipathic projection. With the known structure of the N-terminal domain, we can now reconstruct a model for the Hsp90 dimer and identify key residues involved in ATPase activity and its coupling to the conformational cycle, and in interactions with client proteins and a cochaperone, whose functional significance have been analyzed by mutagenesis in vitro and in vivo.

Results

Crystal Structure

The structure of the 33 kDa middle segment (residues 273–560) of yeast Hsp90 was determined by multiwavelength anomalous dispersion (MAD) using crystals soaked in samarium sulfate, and the structure refined at 2.5 Å resolution (see Experimental Procedures and Table 1). The polypeptide chain is visible from residue 273 to 525 in both molecules in the asymmetric unit, apart from gaps between 377 and 385 in one, and 329 and 338 in the other. A second crystal form with six molecules in the asymmetric unit was refined to 3.0 Å resolution.

The structure can be divided into three regions (Figures 1B and 1C). Residues 273–409 at the start of this segment form a three layer α-β-α sandwich domain consisting of a five-stranded β sheet, a three-turn α helix, and irregular loops on the convex face, and a six-turn α helix nestling in the concavity of the opposite face. Domains with similar folds are found in the MutL DNA

*Correspondence: laurence@icr.ac.uk

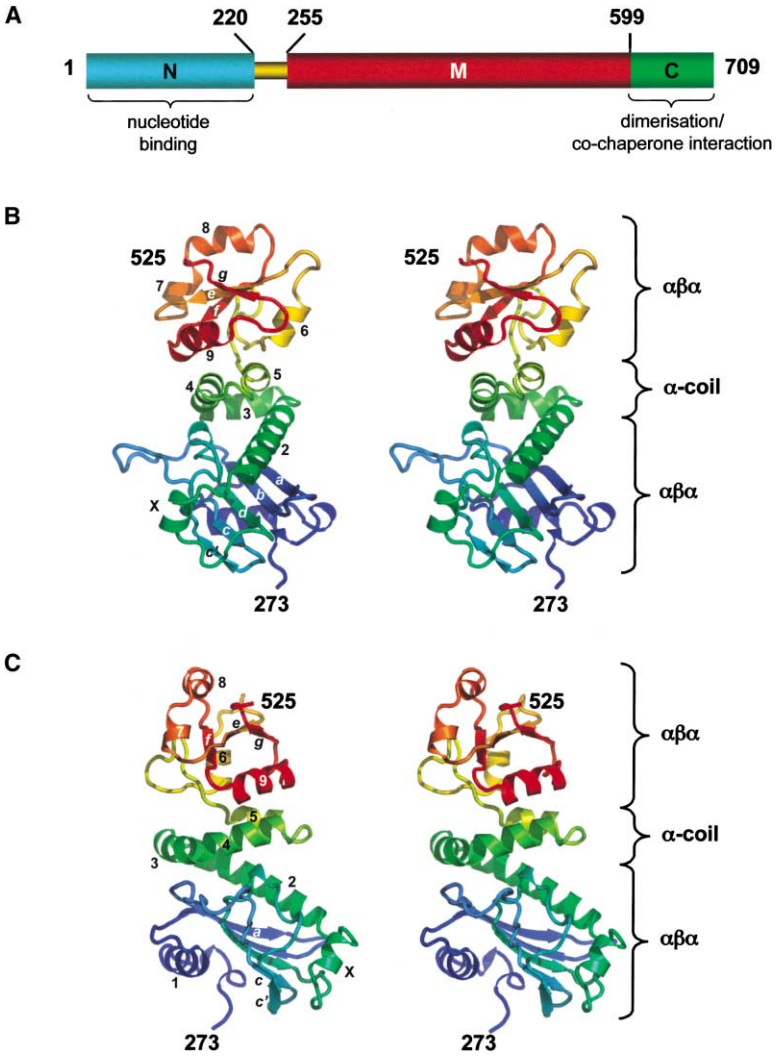

Figure 1. Crystal Structure of Hsp90 Middle Segment

(A) Schematic of Hsp90 structure. The N-terminal nucleotide binding domain (cyan) is linked to the middle segment (red) by a flexible and poorly conserved "charged linker" (yellow).

(B) Stereo pair secondary structure cartoon of the yeast Hsp90 middle segment, rainbow colored (blue to red) from the N to C termini of the construct, showing the two αβα domains linked by an α-helical coil segment. β strands are labeled alphabetically from the N terminus of the construct except for *c′*, which is an additional strand not present in the related MutL and GyrB structures (see below). Helices are numbered from the N terminus of the construct except for X, which has alternative nonhelical conformations.

(C) As (B) but rotated 90° around the vertical.

mismatch repair protein and DNA Gyrase B (GyrB) (see below), both of which also have similar N-terminal ATPase domains to Hsp90, and in the S5 and S9 proteins of the prokaryotic small ribosomal subunit (Wimberly et al., 2000). The long α helix at the C terminus of this domain leads into a small domain formed by three short α helices (411–420, 421–432, and 436–443) arranged in a right-handed coil. This is followed by a third domain (residues 435–525) with a three layer α-β-α sandwich architecture. Although superficially resembling a Rossmann fold, the topology of the secondary structural elements in this domain is quite distinct from previously described α-β-α architectures (Pearl et al., 2000; Murzin et al., 1995), and appears to be a new fold. Beyond residue 525, the structure is disordered. Comparison of the different crystal forms reveals some flexibility in the orientation of the third domain, which shows a rigid body rotation of ~10° with respect to the rest of the structure.

Structural Homology in the GHKL Superfamily

Previous studies (Prodromou et al., 1997a) have shown structural similarity between the N-terminal domain of Hsp90 and those of DNA Gyrase B (Wigley et al., 1991) and MutL (Ban and Yang, 1998), including conservation of residues involved in binding and hydrolysis of ATP in all three systems (Bergerat et al., 1997; Prodromou et al., 1997a; Panaretou et al., 1998; Obermann et al., 1998). Biochemical studies (Prodromou et al., 2000) reinforced that relationship by demonstrating a mechanism of ATP-dependent N-terminal association in the Hsp90 dimer, similar to that described for GyrB (Kampranis et al., 1999). The evolutionary relationship of these systems is further supported by the structure of the middle segment of Hsp90, between the common N-terminal nucleotide binding domain, and the C-terminal dimerization domain whose structure remains unknown in all three systems. Within this segment, residues 273–409 of Hsp90 form a distinct domain with a similar fold to residues 233–375 of GyrB and 207–331 of MutL (Figures 2A–2C). The major differences occur in the polypeptide connecting strands *c′* and *d*, which is a three- to five-turn α helix in GyrB and MutL but a short segment of irregular structure in Hsp90, and between strands *b* and *c*, which is elaborated into a large projecting loop in Hsp90. At the end of the common long helix in this domain, Hsp90 diverges substantially, although there is no structural data for

Table 1. Crystallographic Statistics

Data Set (Crystal Form)	Native (1)	Sm Peak (1)	Sm Edge (1)	Sm Remote (1)	Native (2)
Wavelength (Å)	0.933	1.844	1.845	1.837	0.933
Beamline	ID14-EH2	ID29	ID29	ID29	ID14-EH1
Resolution limit (Å)	2.5	2.7	2.7	2.7	3.0
Observations	28,094	22,146	22,125	22,124	43,645
Completeness (%)	99.9 (99.9)	99.6 (99.3)	99.6 (99.3)	99.4 (99.3)	99.2 (99.2)
Multiplicity	3.6	10.9	3.6	3.6	3.9
Rmerge (%)	8.8 (37.9)	8.8 (46.2)	5.2 (30.7)	5.4 (37.1)	7.6 (29.2)
I/sigI	4.3 (1.9)	6.3 (1.6)	11.1 (2.4)	10.5 (2.0)	7.9 (2.6)
Phasing					
Sites		3	3	3	
Phasing power (iso, ano)		-, 1.9	0.26, 3.87	0.38, 3.58	
MAD <fom>			0.61		
Refinement					
Resolution range (Å)	29.6–2.5				64.5–3.0
No. of reflections	26,622				41,432
No. of protein atoms	4,094				12,314
No. ion atoms	7				13
No. of solvent atoms	199				228
R_{cryst}/R_{free} (%)	24.0/24.7				24.6/32.9
Mean B	72.9				54.3
Rmsd bond lengths (Å)	0.007				0.017
Rmsd bond angles (°)	1.50				1.78

MutL beyond that point. GyrB continues into a seven-turn α helix perpendicular to the preceding helix, which is then the end of the known structure. A topologically equivalent helix is also present in Hsp90, albeit much shorter, and is the first part of the helical coil leading into the second α-β-α sandwich domain.

Reconstructing the Hsp90 Dimer

Structures of C-terminally truncated GyrB and MutL have both been described in ATP-loaded forms in which the clamp is closed and N-terminal domains are associated (Wigley et al., 1991; Ban et al., 1999). The considerable flexibility of the charged "linker" connecting the N-terminal and middle segments has so far prevented this for Hsp90. However, with the structure described here, and the previously described structure of the N-terminal domain of yeast Hsp90 (Prodromou et al., 1997b, 1997a), we are able to construct a model for the "closed" form of the Hsp90 dimer, based on MutL and GyrB, that lacks only the charged linker and the C-terminal dimerization and TPR binding domain (Figure 2E). As there is significant variation between the relative orientations of the N-terminal and middle segments in GyrB and MutL, this Hsp90 dimer model will be inaccurate in detail. Nonetheless, it allows identification of the "inside" and "outside" faces of the middle segment within the dimer, and of regions of the middle segment proximal to the N-terminal domain. On the basis of this reconstruction, we identified three features of the middle segment whose location and structural properties suggested roles in catalyzed ATP hydrolysis, intersegment communication, and client protein interactions (Figures 3A and 3B), and analyzed their involvement by mutagenesis and functional analysis in vivo and in vitro.

Catalytic Loop

The N-terminal domain of Hsp90 provides all the structural requirements for nucleotide binding (Prodromou et al., 1997a) and a catalytic glutamate residue, conserved in MutL and GyrB, which activates the attacking water molecule in the ATPase reaction (Panaretou et al., 1998). However, the N-terminal domain alone has negligible ATPase activity, and in MutL and GyrB, contacts from residues in the middle segment are also required, which "sense" the presence of the γ-phosphate and orientate it for "inline" attack by a nucleophilic water. Both GyrB and MutL contact the γ-phosphate of ATP via a lysine residue (Lys 307 in MutL; Lys 337 in GyrB) on a loop extending from the end of strand *d* in the first sandwich domain of the middle segment. In GyrB, Gln 335 from the same loop hydrogen bonds to the nucleophilic water. Structural alignment with GyrB and MutL identifies the topologically equivalent loop in Hsp90 as Pro 375-Ile 388. Interestingly, this loop contains Glu 381, whose mutation to lysine generates a temperature-sensitive (ts) phenotype in yeast (Nathan and Lindquist, 1995). This segment of polypeptide shows significant conformational flexibility between crystallographically independent views of the molecule (Figure 3C). There is only one lysine residue in this region in Hsp90, Lys 387, but it is not well positioned to act as the equivalent of the catalytic lysines in MutL and GyrB, and is not conserved in the bacterial and mitochondrial Hsp90 homologs HtpG and TRAP1. The conformationally variable "tip" of the loop contains a highly conserved motif: 377- N (L / I /V) S R E x L Q -384, in which the totally conserved Asn 377, Arg 380, and Gln 384 could provide γ-phosphate interactions comparable to those in MutL and GyrB. To test the involvement of these residues, we made mutations in a plasmid-encoded Hsp90 gene in an Hsp90 knockout yeast strain and determined the ability of the mutants to confer viability and activate v-Src in vivo (see Experimental Procedures) (Figure 4 and Table 2). Cells dependent on an Hsp90 allele with an Asn377Ala mutation showed a mild ts phenotype, being viable and competent in v-Src activation at 30°C, but with

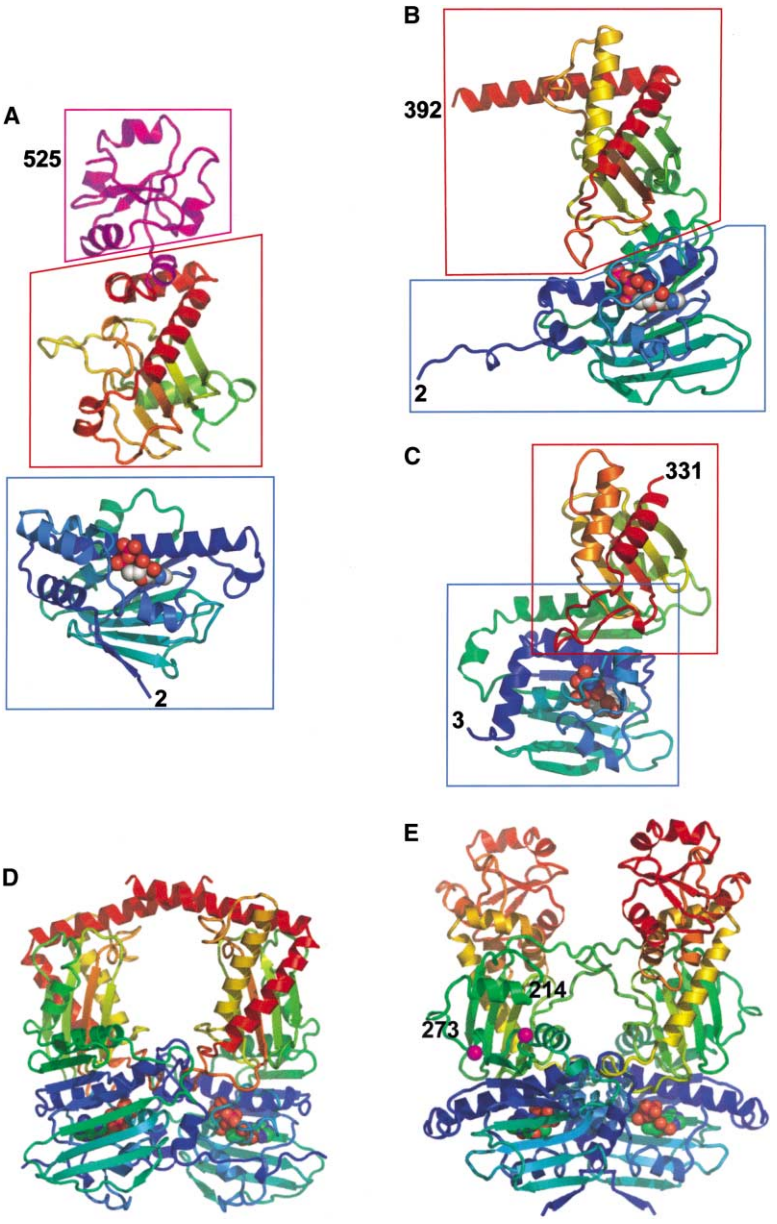

Figure 2. Structural Homology to GyrB and MutL

(A) Structures of yeast Hsp90 monomer from residue 2–525 determined as separate fragments (2–214 and 273–525). The two separately determined structures are shown separated for clarity. The N-terminal domain (blue frame) and first part of the middle segment (red frame) are rainbow colored to correspond to the topologically equivalent structures in GyrB and MutL—the Hsp90-unique domain is colored magenta. The ADP molecule bound to the N-terminal domain of Hsp90, and the AMPPNP bound to GyrB and MutL (see below) are shown as space-filling models.

(B) Secondary structure cartoon of GyrB(2-392) monomer rainbow colored N to C terminus.

(C) Secondary structure cartoon of MutL(2-331) monomer rainbow colored N to C terminus.

(D) Crystal structure of GyrB(2-392) for comparison. The central "hole" running between the jaws of the molecular clamp binds double-stranded DNA during the topoisomerase strand passage reaction.

(E) Model of Hsp90(2-525) dimer reconstructed from the determined structural fragments, structurally aligned with the GyrB(2-392) dimer. By analogy with GyrB, the inner faces of the jaws in the Hsp90 molecular clamp are expected to provide client protein binding site(s). The flexible loops (327–340) projecting from the opposing faces of the clamp come into close proximity in this model and are likely to adopt different conformations in the true dimer.

some growth defects at 37°C. In vitro, Asn377Ala had slightly enhanced ATPase activity at 30°C and 37°C compared to wild-type. In contrast, Hsp90 alleles with Arg380Ala or Gln384Ala mutations were completely incapable of supporting growth at any temperature, indicating complete loss of essential Hsp90 function comparable to that previously seen with mutation of residues involved in ATP binding or hydrolysis in the N-terminal domain (Panaretou et al., 1998). Consistent with this, purified Arg380Ala or Gln384Ala mutant Hsp90s had substantially lower ATPase activities than wild-type protein, in vitro. We also examined the in vitro activity of the ts Glu381Lys mutant (Nathan and Lindquist, 1995). This displayed near wild-type ATPase activity at 30°C, but reduced activation at 37°C. The loss of viability and minimal ATPase activity of the Arg380Ala and Gln384Ala mutants is strong evidence for their direct involvement in catalysis, and together with their location in the Hsp90 structure, suggests that they fulfill the equivalent roles to Lys 337 and Gln 335 in GyrB in orientating the γ-phosphate of ATP. Three ordered conformations for this loop are seen in the two crystal forms of the middle segment; in one of which, Arg 380 and Gln 384 are directed toward the expected position of the N-terminal domain and would be positioned for γ-phosphate interaction (Figure 3C). As there are well-ordered alternative conformations where these groups are not available, efficient catalysis may involve a switch in the conformation of this loop, possibly coupled to client-protein or cochaperone binding.

Intersegment Communication

Unlike GyrB and MutL, where the N-terminal and middle domains are connected by continuous secondary structure (Ban and Yang, 1998; Wigley et al., 1991), N-terminal domain and middle segments in eukaryotic Hsp90s are

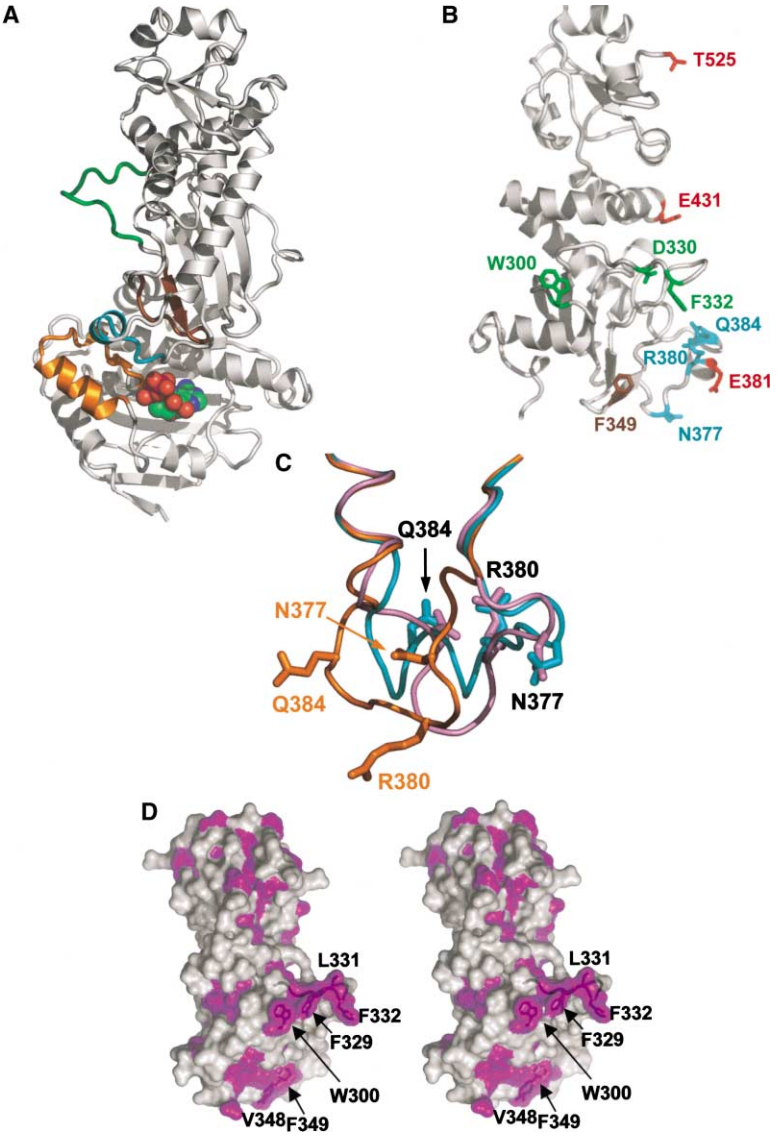

Figure 3. Structural Features of the Hsp90 Middle Segment

(A) One monomer from the reconstructed Hsp90(2-525) model, highlighting the positions of the putative catalytic loop (cyan), the projecting loop (green), and hydrophobic patch (brown) from the middle segment, and the lid (orange) and bound ADP of the N-terminal nucleotide binding domain. The lid is shown in the open conformation observed in crystal structures but is believed to close over the nucleotide on ATP binding.

(B) Location of mutated residues on the middle segment structure. Residues in cyan are in the putative catalytic loop; green are in the projecting loop and adjacent hydrophobic patch; and brown are in the loop and hydrophobic patch directed toward the N-terminal domain in the reconstituted dimer. Residues in red display conditional mutant phenotypes in previous genetic studies (Nathan and Lindquist, 1995; Bohen and Yamamoto, 1993).

(C) Comparison of catalytic loop conformations in three crystallographically independent copies of the middle segment. In one molecule in crystal Form 1 (cyan) the sequence from 380–386 forms a short α helix, with Asn 377 directed away, and Arg 380 and Gln 384 directed toward the body of the structure. In one molecule of crystal Form 2 (pink), the helix has melted to an irregular loop, but the side chains of Asn 377, Arg 380, and Gln 384 remain in the same position as in the helical conformation. In another molecule in Form 2 (gold), the loop is completely remodeled, with Arg 380 and Gln 384 directed toward the predicted position of the N-terminal domain in the dimer, while Asn 377 stabilizes this conformation by hydrogen bonding to the main chain of Gln 384.

(D) Stereo pair of the molecular surface of Hsp90 middle segment with hydrophobic residues highlighted in magenta.

separated by ~50 residues, including an evolutionarily variable and proteolytically labile linker consisting of 20–30 charged amino acids. This linker is dispensable for Hsp90 function in vivo (Louvain et al., 1996) and for ATPase activity in vitro (our unpublished data), and functions primarily as a covalent tether connecting the N-terminal domain to the rest of the protein (Pearl and Prodromou, 2002). Thus, in Hsp90, the link between N-domain and middle segments is very flexible, and their association in the productive ATP-bound state will largely depend on the stability of complementary surface interactions between the domains.

Adjacent to the catalytic loop (see above) we identified a hydrophobic surface "patch" centered on Phe 349 (Figures 3A, 3B, and 3D), near the tip of a loop formed by residues 342–352. Within the Hsp90 dimer model, the side chains of Phe 349 and Val 348 come close to the hydrophobic surfaces believed to be exposed in the N-terminal domain upon nucleotide binding: the exposed face of the "lid" segment (100–123) in its putative closed conformation and the long helix (28–50) carrying the catalytic Glu 33 (Prodromou et al., 2000). This suggests that these conserved accessible hydrophobic residues could be involved in interdomain communication and positioning of the catalytic groups from the N-domain and middle segments. To analyze the role of this patch, we determined the in vivo and in vitro activity of Phe349Ala and Phe349Gln mutants. Both mutations generated growth defects in vivo, with the more radical substitution Phe349Gln showing severe effects. Both mutants were substantially defective in v-Src activation in vivo and displayed very low ATPase activity in vitro (Figure 4 and Table 2).

Client Protein Binding Sites

Mutagenesis studies of GyrB implicate basic residues on the inside face of the middle domain in functional interactions with DNA bound in the clamp (Tingey and Maxwell, 1996). While GyrB and Hsp90 have very different functions, they have related structures and comparable ATPase-coupled molecular clamp mechanisms, suggesting that binding sites for their macromolecular

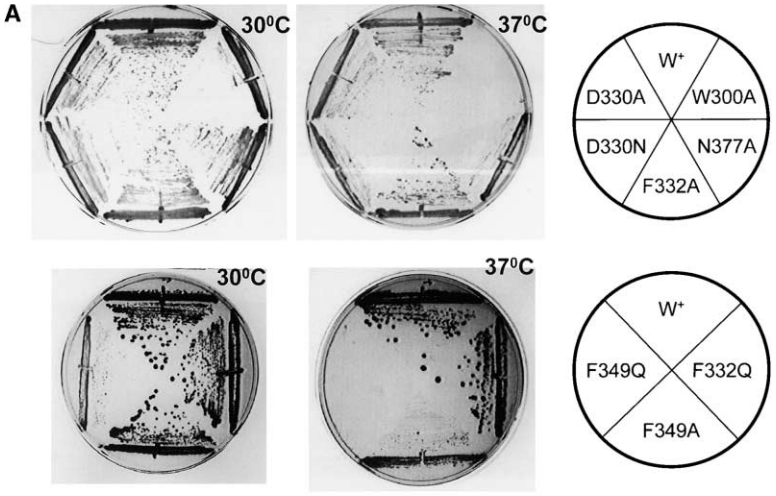

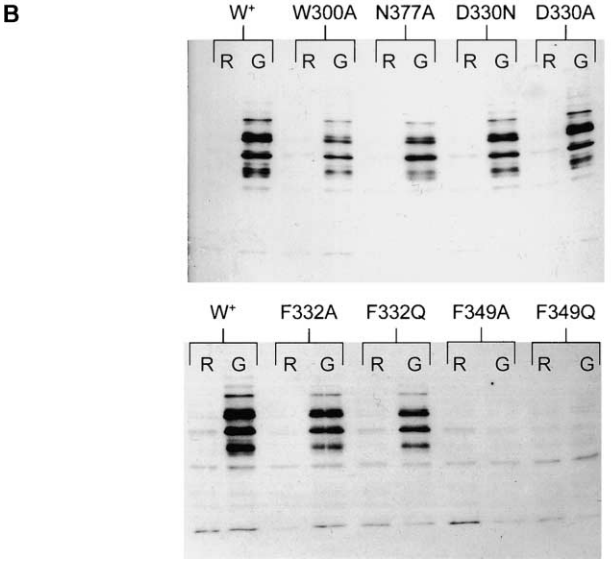

Figure 4. Functional Analysis of Middle Segment Features

(A) Growth of middle segment mutants on rich medium (see Experimental Procedures) at 30°C and 37°C degrees. Plates were incubated long enough to minimally visualize the poorest growing but still viable mutants. Relative growth of mutants is shown in Table 2.
(B) Ability of middle segment mutants to chaperone v-Src, visualized by introduction of phospho-tyrosine into yeast proteins. v-Src induction was triggered by transfer of cultures from raffinose medium (R), which represses v-Src transcription, to galactose medium (G), which induces it.

ligands (DNA or client protein) might have similar locations in the structure. The inner faces of the middle segment of Hsp90 possess some interesting features, including an exposed hydrophobic patch, which could play a role in protein-protein interactions (Figures 3A, 3B, and 3D). This patch involves the side chains of Trp 300, and Phe 329, Leu 331, and Phe 332, which form one side and the tip of a conformationally flexible loop, cantilevered out from the main body of the structure. This solvent-exposed loop has an unusual sequence

Table 2. Phenotypes, Client Protein Activation, and ATPase Activity of Hsp90 Middle Segment Mutants

	Cell Growth		v-Src Activation	ATPase min^{-1}	
Genotype	30°C	37°C	30°C	30°C	37°C
Wild-type	++++	++++	++++	0.26	0.83
N377A	++++	+	++	0.30	1.12
R380A	-	-	-	0.017	0.018
E381K	N/D	N/D	N/D	0.29	0.52
Q384A	-	-	-	0.062	0.15
W300A	+	-	+	0.51	1.15
D330A	+++	+++	++++	0.19	0.51
D330N	+++	+	+++	0.25	0.59
F332A	++++	++++	+++	0.34	0.93
F332Q	++++	+++	++	0.34	0.86
F349A	++	+	-	0.005	0.023
F349Q	+	-	-	0.028	0.099

(327-A P F D L F E S K K K K N N-340) generating an amphipathic structure, with one hydrophobic side and one positively charged side.

To gain some insight into the function of this feature, we analyzed the effect on Hsp90 function in vivo and in vitro of mutations of the exposed hydrophobic residues Trp 300 and Phe 332, and of Asp 330, which is involved in polar interactions across the loop (Figure 4 and Table 2). Mutation of Phe 332 had relatively little effect in vivo, with Phe332Ala nearly wild-type, although Phe332Gln showed slight temperature sensitivity and decrease in v-Src activation. In vitro, both Phe 332 mutants retained significant ATPase activity. Asp 330 mutants also displayed in vitro ATPase activity comparable to wild-type, and near wild-type growth and v-Src activation at 30°C, although Asp330Asn showed some growth defects at 37°C. In contrast, the Trp300Ala mutant, which retained substantial ATPase activity in vitro, showed severe defects in growth and v-Src activation at 30°C and was not viable at 37°C. The segment of Hsp90 connecting Trp 300 and the projecting loop, and partially overlapping the beginning of that loop, was found to be required for Hsp90 interaction with the client protein PKB/Akt (Sato et al., 2000). As the Trp300Ala mutant has a functional ATPase, it is likely that its inadequacy as a chaperone in vivo results from a defect in client protein activation and implicates Trp 300 in client protein interaction.

Previous in vivo studies identified other positions where ts mutations affected Hsp90-dependent activation of client proteins, some of which map to the middle segment (Figure 3B). Gly 313 occupies a conformationally restricted position at the tip of a β hairpin in the first domain of the middle segment, and its mutation to asparagine (Bohen and Yamamoto, 1993; Nathan and Lindquist, 1995) would generate a generally destabilizing structural defect. Glu341Lys, identified in a screen for mutants defective in glucocorticoid receptor activation (Bohen and Yamamoto, 1993), maps to the middle helix in the helical coil connecting the two α-β-α sandwich domains. Thr525Ile lies at end of the presently visible structure, as the peptide chain emerges from the second α-β-α sandwich domain. Glu341 and Thr 525 present on the same face as Trp 300 and the 327–340 projecting loop. Although the ATPase activity of the Glu341Lys and Thr525Ile mutants has not been determined, their location suggests that their functional impairment in vivo results from defects in client protein interaction rather than ATP hydrolysis.

Aha1 Interactions

Hsp90 function involves a range of cochaperone proteins which facilitate client protein loading and regulate progress through the chaperone cycle (reviewed in Pearl and Prodromou, 2002). Recently we characterized a new family of Hsp90 cochaperones, Hch1/Aha1, which contribute to Hsp90 function in vivo, and bind to Hsp90 and stimulate its ATPase activity in vitro (Panaretou et al., 2002). Unlike TPR domain cochaperones and the kinase-specific cochaperone Cdc37p/p50^{cdc37}, Aha1 does not compete for binding to the C-terminal domain of Hsp90 (Owens-Grillo et al., 1996; Silverstein et al., 1998) and can coexist in complexes with Sti1 and Cpr6. The prototype of this family, Hch1, was discovered as a high copy number suppressor of an Hsp90 mutant allele, Glu381Lys (Nathan and Lindquist, 1995). The location of this residue in the catalytic loop bearing Arg 380 and Gln 384 (see above) suggested that the middle segment of Hsp90 might be involved in direct interaction with Hch1 and/or Aha1, and this was confirmed by coprecipitation and isothermal titration calorimetry (Figure 5A). To probe the mechanism of Aha1 action, we determined the effect of some of the mutations described above, on the ability of Aha1 to stimulate the ATPase activity of Hsp90. Mutation of Asp 330 in the projecting loop, which had minimal effect on the inherent ATPase activity of Hsp90 also had little effect on activation by Aha1. Within the catalytic loop, the Arg380Ala and Gln384Ala mutants that had greatly diminished inherent ATPase activity showed negligible activation by Aha1 consistent with their direct involvement in the hydrolysis reaction. The Glu381Lys mutant, with near wild-type activity at 30°C, was significantly impaired in its response to Aha1, showing ~10-fold lower activation than wild-type. In contrast, the Phe 349 mutants with severely impaired ATPase activities were responsive to Aha1 activation, being stimulated to ~30% of the wild-type activity at comparable Aha1 concentrations. Analyzed in terms of fold activation over the inherent activity, the Phe 349 mutants were found to be hyperresponsive to Aha1, being stimulated by more than 80-fold over the basal activity, at saturation (data not shown).

Discussion

The accumulating structural and biochemical data suggest that like GyrB and MutL, Hsp90 is a "split" ATPase in which catalytic groups from independent domains in the same molecule come together to achieve ATP hydrolysis. With the structure presented here, we are able to identify Arg 380 and Gln 384 as probable catalytic residues contributed by the middle segment of Hsp90, and have confirmed their essential involvement in ATPase activity in vitro and chaperone function in vivo. The "catalytic loop" bearing Arg 380 and Gln 384 shows significant conformational plasticity, varying between a helical structure where the catalytic residues are directed back into the middle segment, to an extended loop in which they could reach "down" into the ATP binding site in the N terminus (Figures 3A and 3B). Unlike GyrB and MutL, the N-terminal domain and middle segment of Hsp90 are separated by an evolutionarily variable and extremely flexible linker segment, which tethers the loosely associated segments to each other.

The lid segment in the N-terminal domain of Hsp90 is also very different from the short flexible lids of GyrB and MutL, consisting of a helix-loop-helix segment which is fully ordered in the absence or presence of bound nucleotide, and which makes extensive hydrophobic interactions in its openconformation. Mechanistic analogy with GyrB and MutL requires that the lid closes on binding of ATP, and mutagenesis studies suggest this does indeed occur (Prodromou et al., 2000), but it has not yet been observed directly. Lid closure would expose the hydrophobic surface buried underneath the lid in its open conformation, and the juxtaposed hydrophobic face of the lid itself. In the absence

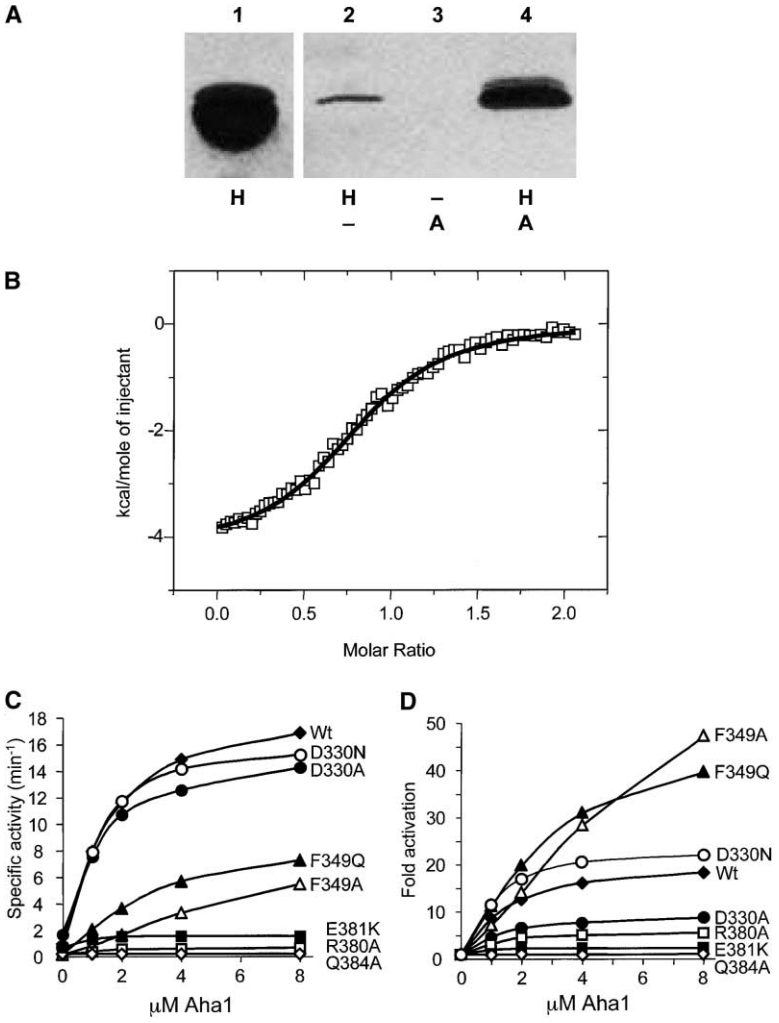

Figure 5. Middle Segment Interaction with the Activating Cochaperone Aha1

(A) Coprecipitation of Hsp90 middle segment (273–560) by the N-terminal Hsp90 binding domain of yeast Aha1 (nAha1). Lane 1: Hsp90(273-560) positive control; lanes 2–4: talon bead coprecipitations (H = Hsp90(273-560); A = nAha1). All lanes are visualized with polyclonal Ab to yeast Hsp90. Some weak nonspecific binding of Hsp90(273-560) to beads is visible in lane 2, but there is very substantial coprecipitation of Hsp90(273-560) when His_6-tagged nAha1 is included (lane 4).

(B) Isothermal titration calorimetry of Hsp90(273–560) binding to full-length Aha1. The fitted curve is superimposed on the experimental points (open squares). The proteins interact with a K_D of 2.9 ± 0.3 μM and a stoichiometry of ~1:1.

(C) Stimulation of the inherent ATPase activity of wild-type and yeast Hsp90, and middle segment mutants. Mutations in projecting loop (D330N/A) had little effect on activation by Aha1. Catalytic loop mutants (R380A, Q384A) lacking ATPase activity were not reactivated by Aha1, but E381K, which displays near wild-type activity rendered Hsp90 resistant to Aha1 activation. The intersegment communication patch mutants (F349Q/A), which lack ATPase activity in isolation, were very substantially reactivated by Aha1.

(D) Data as in (B) but replotted in terms of fold activation over the basal activity of each Hsp90 variant in the absence of Aha1. The substantial sensitivity of the Phe 349 mutants to Aha1 stimulation, is clearly seen.

of compensating interactions, exposure of these surfaces would be unfavorable and present an energetic barrier to lid closure. Within the Hsp90 dimer, the exposed surface beneath the lid from one monomer can bury the equivalent from the other, and drive ATP-dependent association of the N-terminal domains (Prodromou et al., 2000; Chadli et al., 2000). The exposed surface of the closed lid could interact with the middle segment of the same monomer, and we have identified a hydrophobic patch, centered on Phe 349, that could participate in that intersegment interaction. Mutation of Phe 349 produced a very substantial loss of ATPase activity consistent with that role. Efficient ATP hydrolysis in Hsp90 appears to require a series of conformational changes that together conspire to the "rate-limiting" step of the hydrolysis reaction. Thus, ATP binding promotes lid closure, which is stabilized by dimeric association of the N-terminal domains, and association between the N-terminal and middle segments. A second conformational "switch" event may also occur in which the catalytic loop of the middle segment melts from an inactive helical conformation to direct the catalytic residues toward the γ-phosphate of the ATP. Within this complex set of events, the recently described Hsp90 cochaperone Aha1 (Panaretou et al., 2002) achieves its effect of activating the ATPase. Mutation of Glu 381 within the catalytic loop had no effect on the basal ATPase of Hsp90, but rendered it almost completely insensitive to Aha1 stimulation. Mutation of Phe 349 within the hydrophobic patch implicated in intersegment communication caused a very significant loss of ATPase activity, but this was hypersensitive to activation by Aha1. Taken together, these observations suggest that Aha1 might function by facilitating the interaction between the middle segment and ATP-bound conformation of the N-terminal domain, and implicates Glu 381 in mediating that function (Figure 6).

How Hsp90 can interact specifically and selectively with its protein "clientele" remains the major conundrum in the field, and as yet there is no consensus even as to which part (or parts) of the Hsp90 structure mediates those interactions. The architectural similarity and common ATPase-coupled clamp mechanism of Hsp90 and GyrB suggests that as with DNA binding by GyrB, productive binding of client proteins by Hsp90 involves the opposing inner faces of the middle segments in the closed conformation of the clamp. In the structure of the middle segment, we have identified candidate features for client-protein interaction, in particular the projecting loop and associated hydrophobic patch in the

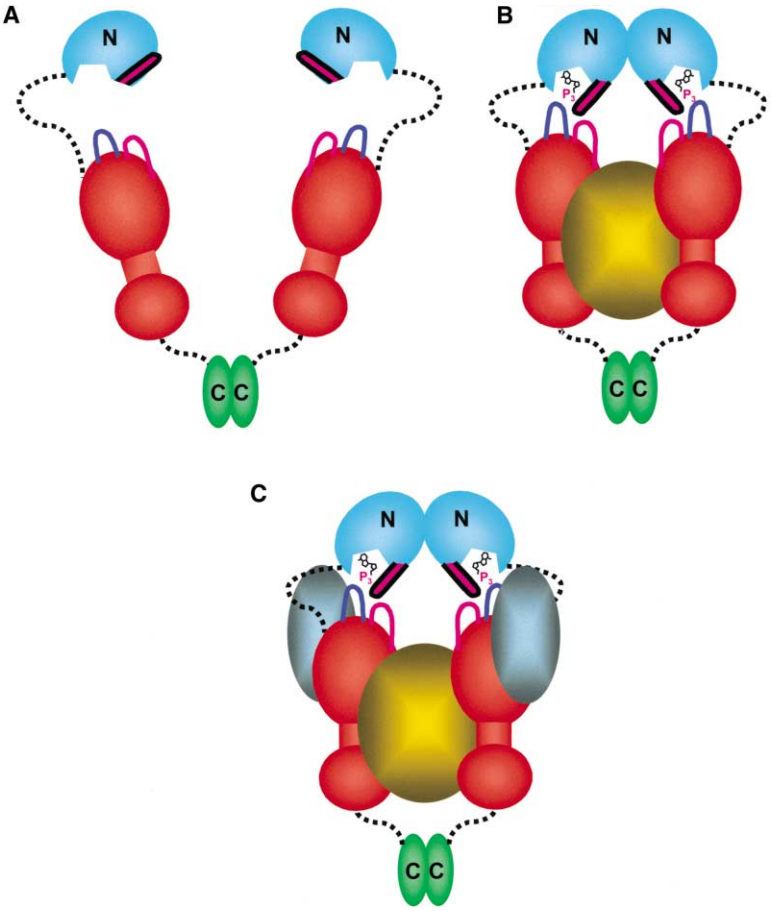

Figure 6. Model of the Hsp90 ATP-Dependent Molecular Clamp Mechanism

(A) Hsp90 dimer in a "relaxed" state in the absence of ATP. The lid (black and magenta) in the N-terminal nucleotide binding domain is open, and the N-terminal domains are not constrained.

(B) Binding of ATP causes lid closure, exposing a hydrophobic patch on the N-domain which associates with the equivalent in the other monomer. The exposed face of the lid itself is stabilized by interaction with a hydrophobic patch from the middle segment (magenta loop), which provides catalytic residues for the ATP-hydrolytic reaction (blue loop). The closed "tense" form interacts with client proteins (gold) to facilitate their activation and/or assembly with ligands, but how this occurs at the biochemical level is unknown.

(C) Aha1 (gray) interacts with the middle segment and speeds up the ATPase reaction, possibly by stabilizing interactions between the middle and N-terminal domain(s).

first domain. Although mutations in the loop itself only had mild effects, mutation of an adjacent exposed hydrophobic residue caused substantial impairment of chaperone function in vivo without loss of ATPase activity in vitro, suggesting a defect in client protein interaction. In support of this interpretation, this region coincides with a segment of Hsp90 found to be essential for mediating interaction with an authentic client, PKB/Akt, in a yeast two-hybrid assay (Sato et al., 2000). As client proteins interact with Hsp90 in a substantially folded state, they are unlikely to present extensive hydrophobic surfaces for interaction with Hsp90. Instead, the projecting loop of Hsp90 may provide a flexible amphipathic "finger" that can insert into clefts and crevices between the folded domains of the client protein.

The second $\alpha\beta\alpha$ domain of the middle segment of Hsp90 has recently been implicated in binding to the client protein eNOS (Fontana et al., 2002). Intriguingly, PKB/Akt and eNOS were able to bind simultaneously to the middle segment of Hsp90, which appeared able to "scaffold" their interaction and facilitate phosphorylation of eNOS by PKB/Akt. The possibility that Hsp90 interacts with two different client proteins simultaneously has interesting implications, as there are several signaling pathways in which consecutive pairs of interacting proteins are both Hsp90 clients. For example, in the eNOS activation pathway, as well as PKB/Akt and eNOS, the upstream activator of PKB/Akt, PDK1 is also an Hsp90 client (Fujita et al., 2002). Other examples include the mitogenic signaling cascade in which Mek, its activating kinase Raf, and its activating kinase c-Src are all Hsp90 clients (Pratt, 1998; Setalo et al., 2002; Stancato et al., 1993; Xu et al., 1999), and the yeast cyclin-dependent kinase Cdc28 and its activating kinase Cak1 (Farrell and Morgan, 2000). Thus, as well as its function as a chaperone, protecting its clients from inappropriate liaisons, multiple client binding sites in the middle segment may allow Hsp90 the more proactive role of matchmaker, facilitating productive interactions between them.

Experimental Procedures

Expression, Purification, and Crystallization of the Middle Segment of Hsp90

A stable middle segment of yeast Hsp90(260-551) was defined by limited proteolysis and a series of constructs with variation of the N and C terminus were cloned with protease-cleavable N-terminal His_6 tags into pRSETA and expressed in *E. coli* BL21(DE3) pLysS. Expressed protein was purified by Talon metal affinity chromatography, ion exchange on Q-Sepharose, and size-exclusion chromatography on a Superdex 75 PG column. Purified protein was dialyzed into 20 mM Tris-HCl (pH 7.5), 1 mM EDTA, and 0.5 mM DTT and concentrated.

Crystals for several constructs were obtained, but useful diffraction was only observed for a construct comprising residues 273–560 from which the N-terminal His tag had been removed by proteolysis. High-quality crystals (Form 1) obtained from this construct grew from 24 mg/ml protein in a buffer containing 11 mM $CdSO_4$, 20 mM $MgCl_2$, 80 mM Tris-HCl (pH 7.5), and 5% v/v glycerol in under-oil microbatch experiments at 14°C. A second crystal form (Form 2)

was obtained with the same construct in a similar buffer containing 67 mM $CdSO_4$ and 10 mM ADP.

Crystallographic Data Collection, Phasing, and Refinement

Crystals of yeast Hsp90(273-560) were cryoprotected in crystallization buffer with 10% glycerol and 8% 2,3-butanediol and flash cooled in liquid nitrogen. Crystals of Form 1 have space group $P6_1$ with unit cell dimensions a = b = 112.88 Å, c = 112.59 Å, suggesting a solvent content of 62% with two molecules in the asymmetric unit. This was supported by the observation of a noncrystallographic 2-fold axis in self-rotation functions. Derivatives were obtained by soaking native crystals for 1 hr in cryoprotectant buffer containing 0.1 mM $SmSO_4$. A three wavelength MAD dataset was collected on beamline ID29 at the ESRF Grenoble. Image processing and data reduction used MOSFLM (Leslie, 1995) and SCALA (CCP4, 1994). Phases were calculated with SOLVE (Terwilliger and Berendzen, 1999) and refined with SHARP (de la Fortelle and Bricogne, 1997) and RESOLVE (Terwilliger, 2000), to give a map of very high quality in which the majority of the structure was built using TURBO (Roussel and Cambillau, 1991). The resulting structure was refined using CNS (Brunger et al., 1998) and REFMAC (Murshudov et al., 1997) together with manual correction with TURBO.

Form 2 crystals also have space group $P6_1$ but with unit cell dimensions a = b = 192.64 Å, c = 106.08 Å, suggesting a solvent content of 58% with six molecules in the asymmetric unit. Statistics for data collections, phasing, and refinements are given in Table 1. Coordinates and structure factors have been deposited in the Protein DataBank with PDB Code 1HK7.

Expression, Purification, and ATPase Assay of Hsp90 Mutants

Proteins expressed as His_6-tagged fusions were purified as described previously using Talon metal-affinity chromatography, Q-Sepharose ion exchange and Sephacryl 400HR gel filtration chromatography (Panaretou et al., 1998). Proteins were concentrated in 20 mM Tris, pH 7.5, containing 0–25 mM NaCl, 1 mM EDTA, and 0.5 mM DTT. The Hsp90 ATPase assay was performed as previously described (Panaretou et al., 1998), except that the assay conditions were modified (45 mM Tris-HCl, pH 7.5, 9 mM KCl, and 3 mM $MgCl_2$), and for the Aha1 assays 20 mM Tris-HCl, pH 7.5, 4 mM KCl, and 1.2 mM $MgCl_2$ was used.

In Vivo Analysis of Mutants

Single amino acid changes were generated in the yeast *HSP82* coding sequence in pRSETA-90 (Prodromou et al., 2000) using the QuickChange site-directed mutagenesis kit (Stratagene) and confirmed by dye terminator cycle sequencing. For expression in yeast, coding sequences were PCR amplified from the *E. coli* plasmids and inserted between the *HSC82* promoter and *ADH1* terminator in the *E.coli/S.cerevisiae* LEU2 shuttle vector pHSCprom (Panaretou et al., 1999). *HSP82* mutant alleles were expressed in *S. cerevisiae* strain PP30 (Panaretou et al., 1998). In this strain, the genomic copy of both *HSP82* and *HSC82* are deleted, and essential Hsp90 function is provided by wild-type *HSC82* expressed from a *URA3* vector. PP30 was transformed with vectors bearing wild-type or mutant *HSP82* and transformants selected on dropout media. Ability of *HSP82* mutants to maintain cell viability was assessed by streaking on dropout media without leucine, but containing uracil (50 mg/l) and 5-fluoroorotic acid (0.1%). Mutants that maintained viability, once cured of the *URA3* vector expressing *HSC82*, were streaked on dropout media containing uracil, but without leucine, to compare growth rates with cells expressing wild-type *HSP82*. Cells were also streaked on rich, nonselective media (YPD; 2% glucose, 2% bactopeptone, 15 yeast extract, and 2% agar).

In Vivo v-Src Activation Assays

PP30 cells expressing various *HSP82* mutant alleles were transformed with the centromeric *URA3* vector, YpRS316v-Src (Murphy et al., 1993; Nathan et al., 1999) expressing v-Src under control of the GAL1 promoter. Transformed cells were grown at 30°C to exponential phase in synthetic raffinose (SR) medium (2% raffinose, 0.67% yeast nitrogen base without amino acids, 2% agar, and supplemented with appropriate amino acids and without uracil), harvested, and resuspended in 10 ml SR without carbon source. Subsequently, 5 ml aliquots were transferred into SR and SGa (as SR but with 2% galactose in place of raffinose), incubated at 30°C for 6 hr, harvested, and lysed as previously described (Panaretou et al., 1998), except for inclusion of 0.2 mM sodium orthovanadate in the extraction buffer. Lysates fractionated by 12.5% SDS-PAGE were transferred to nitrocellulose membrane, and phosphotyrosine-labeled protein was detected with 4G10 anti-phosphotyrosine Ab (Upstate), followed by affinity-purified goat anti-mouse HRP linked Ab and visualized by ECL (Amersham-Pharmacia).

Aha1-Hsp90 Interactions

Interaction between yeast Aha1 and Hsp90 was analyzed qualitatively by coprecipitation of Hsp90(273-560) with an N-terminal domain of Aha1 (nAha1) previously shown to stimulate Hsp90 ATPase (Panaretou et al., 2002). 50 μg of purified His-tagged nAha1 was incubated with the same amount of Hsp90 central segment at 4°C for 30 min in a buffer containing 20 mM Tris-HCl, pH 7.5, 50 mM NaCl, and 0.1% Nonidet P-40. 20 μl of Talon beads (Clontech) was then added and the reaction incubated for another 30 min at 4°C. The beads were washed twice with the same buffer on Costar spin filters. 20 μl of SDS-PAGE loading buffer was added to the beads, and 15 μl was loaded on SDS-PAGE gels for blotting onto nitrocellulose filters. Blots were probed with rabbit polyclonal anti-Hsp90 followed by anti-rabbit HRP conjugated secondary Ab to allow detection with ECL kit (Amersham-Pharmacia).

Quantitative analysis was perfomed by isothermal titration calorimetry, on an MSC system (Microcal Inc., MA). 140 μM aliquots of 8 μl of Hsp90(273-560) were injected in 1.458 ml of 32.4 μM Aha1 at 25°C in a buffer containing 20 mM Tris-HCl, pH 7.5, 1 mM EDTA. After subtracting the heats of dilution, determined in a separate experiment by diluting protein into buffer, the resulting data were fitted using a nonlinear least square curve-fitting algorithm (Microcal Origin) with three floating variables: stoichiometry, binding constant, and change of enthalpy of interaction.

Acknowledgments

This work was supported by the Wellcome Trust (L.H.P.), Medical Research Council (L.H.P.), and University of London Central Research Fund (B.P.). B.H. gratefully acknowledges the support of the K.C. Wong Education Foundation and China Scholarship Council. We are very grateful to William Shepard and Gordon Leonard of beamline ID29 (ESRF Grenoble) for assistance with data collection. B.H. is a visiting Doctoral Scholar from the College of Life Science, Zhejiang University, China.

Received: October 23, 2002
Revised: December 24, 2002

References

Ban, C., and Yang, W. (1998). Crystal structure and ATPase activity of MutL: implications for DNA repair and mutagenesis. Cell *95*, 541–552.

Ban, C., Junop, M., and Yang, W. (1999). Transformation of MutL by ATP binding and hydrolysis: a switch in DNA mismatch repair. Cell *97*, 85–97.

Bergerat, A., de Massy, B., Gadelle, D., Varoutas, P.C., Nicolas, A., and Forterre, P. (1997). An atypical topoisomerase II from Archaea with implications for meiotic recombination. Nature *386*, 414–417.

Bohen, S.P., and Yamamoto, K.R. (1993). Isolation of Hsp90 mutants by screening for decreased steroid receptor function. Proc. Natl. Acad. Sci. USA *90*, 11424–11428.

Brunger, A.T., Adams, P.D., Clore, G.M., DeLano, W.L., Gros, P., Grosse-Kunstleve, R.W., Jiang, J.S., Kuszewski, J., Nilges, M., Pannu, N.S., et al. (1998). Crystallography & NMR system: A new software suite for macromolecular structure determination. Acta Crystallogr. D *54*, 905–921.

CCP4 (Collaborative Computational Project 4) (1994). The CCP4 suite: programs for protein crystallography. Acta Crystallogr. D *50*, 760–763.

Chadli, A., Bouhouche, I., Sullivan, W., Stensgard, B., McMahon, N.,

Catelli, M.G., and Toft, D.O. (2000). Dimerization and N-terminal domain proximity underlie the function of the molecular chaperone heat shock protein 90. Proc. Natl. Acad. Sci. USA *97*, 12524–12529.

Chavany, C., Mimnaugh, E., Miller, P., Bitton, R., Nguyen, P., Trepel, J., Whitesell, L., Schnur, R., Moyer, J., and Neckers, L. (1996). p185erbB2 binds to GRP94 in vivo. Dissociation of the p185erbB2/GRP94 heterocomplex by benzoquinone ansamycins precedes depletion of p185erbB2. J. Biol. Chem. *271*, 4974–4977.

Clarke, P.A., Hostein, I., Banerji, U., Stefano, F.D., Maloney, A., Walton, M., Judson, I., and Workman, P. (2000). Gene expression profiling of human colon cancer cells following inhibition of signal transduction by 17-allylamino-17- demethoxygeldanamycin, an inhibitor of the hsp90 molecular chaperone. Oncogene *19*, 4125–4133.

de la Fortelle, E., and Bricogne, G. (1997). Maximum-likelihood heavy-atom parameter refinement for multiple isomorphous replacement and multiwavelength anomalous diffraction methods. In Macromolecular Crystallography Part A, C.W. Carter and R.M. Sweet, eds. (San Diego: Academic Press), pp. 472–494.

Farrell, A., and Morgan, D.O. (2000). Cdc37 promotes the stability of protein kinases Cdc28 and Cak1. Mol. Cell. Biol. *20*, 749–754.

Fontana, J., Fulton, D., Chen, Y., Fairchild, T.A., McCabe, T.J., Fujita, N., Tsuruo, T., and Sessa, W.C. (2002). Domain mapping studies reveal that the M domain of hsp90 serves as a molecular scaffold to regulate Akt-dependent phosphorylation of endothelial nitric oxide synthase and NO release. Circ. Res. *90*, 866–873.

Fujita, N., Sato, S., Ishida, A., and Tsuruo, T. (2002). Involvement of Hsp90 in signaling and stability of 3- phosphoinositide-dependent kinase-1. J. Biol. Chem. *277*, 10346–10353.

Grenert, J.P., Sullivan, W.P., Fadden, P., Haystead, T.A.J., Clark, J., Mimnaugh, E., Krutzsch, H., Ochel, H.-J., Schulte, T.W., Sausville, E., et al. (1997). The amino-terminal domain of heat shock protein 90 (hsp90) that binds geldanamycin is an ATP/ADP switch domain that regulates hsp90 conformation. J. Biol. Chem. *272*, 23843–23850.

Grenert, J.P., Johnson, B.D., and Toft, D.O. (1999). The importance of ATP binding and hydrolysis by Hsp90 in formation and function of protein heterocomplexes. J. Biol. Chem. *274*, 17525–17533.

Kampranis, S.C., Bates, A.D., and Maxwell, A. (1999). A model for the mechanism of strand passage by DNA gyrase. Proc. Natl. Acad. Sci. USA *96*, 8414–8419.

Leslie, A.G.W. (1995). MOSFLM Users Guide (Cambridge, UK: MRC Laboratory of Molecular Biology).

Louvain, J.-F., Warth, R., and Picard, D. (1996). The eukaryote-specific regions of Hsp82 are dispensible for its viability and signal transduction functions in yeast. Proc. Natl. Acad. Sci. USA *93*, 13937–13942.

Murphy, S.M., Bergman, M., and Morgan, D.O. (1993). Suppression of C-Src activity by C-terminal Src kinase involves the C-Src Sh2-(D)OMAIN and Sh3-domain: analysis with Saccharomyces cerevisiae. Mol. Cell. Biol. *13*, 5290–5300.

Murshudov, G.N., Vagin, A.A., and Dodson, E.J. (1997). Refinement of macromolecular structures by the maximum-likelihood method. Acta Crystallogr. D *53*, 240–255.

Murzin, A.G., Brenner, S.E., Hubbard, T., and Chothia, C. (1995). SCOP: a structural classification of proteins database for the investigation of sequences and structures. J. Mol. Biol. *247*, 536–540.

Nathan, D.F., and Lindquist, S. (1995). Mutational analysis of Hsp90 function: interactions with a steroid receptor and a protein kinase. Mol. Cell. Biol. *15*, 3917–3925.

Nathan, D.F., Vos, M.H., and Lindquist, S. (1997). *In vivo* functions of the *Saccharomyces cerevisiae* Hsp90 chaperone. Proc. Natl. Acad. Sci. USA *94*, 12949–12956.

Nathan, D.F., Vos, M.H., and Lindquist, S. (1999). Identification of SSF1, CNS1, and HCH1 as multicopy suppressors of a *Saccharomyces cerevisiae* Hsp90 loss-of-function mutation. Proc. Natl. Acad. Sci. USA *96*, 1409–1414.

Obermann, W.M.J., Sondermann, H., Russo, A.A., Pavletich, N.P., and Hartl, F.U. (1998). *In vivo* function of Hsp90 is dependent on ATP binding and ATP hydrolysis. J. Cell Biol. *143*, 901–910.

Owens-Grillo, J.K., Czar, M.J., Hutchinson, K.A., Hoffman, K., Perdew, G.H., and Pratt, W.B. (1996). A model of protein targetting mediated by immunophilins and other proteins that bind to hsp90 via tetratricopeptide repeat domains. J. Biol. Chem. *271*, 13468–13475.

Panaretou, B., Prodromou, C., Roe, S.M., O'Brien, R., Ladbury, J.E., Piper, P.W., and Pearl, L.H. (1998). ATP binding and hydrolysis are essential to the function of the Hsp90 molecular chaperone *in vivo*. EMBO J. *17*, 4829–4836.

Panaretou, B., Sinclair, K., Prodromou, C., Johal, J., Pearl, L.H., and Piper, P.W. (1999). The Hsp90 of *Candida albicans* can confer Hsp90 functions in *Saccharomyces cerevisiae*: a potential model for the processes that generate immunogenic fragments of this molecular chaperone in *C.albicans* infections. Microbiology *145*, 3455–3463.

Panaretou, B., Siligardi, G., Meyer, P., Maloney, A., Sullivan, J.K., Singh, S., Millson, S.H., Clarke, P.A., Naaby-Hansen, S., Stein, R., et al. (2002). Activation of the ATPase activity of Hsp90 by the stress-regulated cochaperone Aha1. Mol. Cell, *10*, 1307–1318.

Pearl, L.H., and Prodromou, C. (2002). Structure, function and mechanism of the Hsp90 molecular chaperone. Adv. Protein Chem. *59*, 157–185.

Pearl, F.M.G., Lee, D., Bray, J.E., Sillitoe, I., Todd, A.E., Harrison, A.P., Thornton, J.M., and Orengo, C.A. (2000). Assigning genomic sequences to CATH. Nucleic Acids Res. *28*, 277–282.

Pratt, W.B. (1998). The hsp90-based chaperone system: involvement in signal transduction from a variety of hormone and growth factor receptors. Proc. Soc. Exp. Biol. Med. *217*, 420–434.

Prodromou, C., Piper, P.W., and Pearl, L.H. (1996). Expression and crystallisation of the yeast Hsp82 chaperone, and preliminary X-ray diffraction studies of the amino-terminal domain. Proteins Struct. Funct. Genet. *25*, 517–522.

Prodromou, C., Roe, S.M., O'Brien, R., Ladbury, J.E., Piper, P.W., and Pearl, L.H. (1997a). Identification and structural characterization of the ATP/ADP-binding site in the Hsp90 molecular chaperone. Cell *90*, 65–75.

Prodromou, C., Roe, S.M., Piper, P.W., and Pearl, L.H. (1997b). A molecular clamp in the crystal structure of the N-terminal domain of the yeast Hsp90 chaperone. Nat. Struct. Biol. *4*, 477–482.

Prodromou, C., Panaretou, B., Chohan, S., Siligardi, G., O'Brien, R., Ladbury, J.E., Roe, S.M., Piper, P.W., and Pearl, L.H. (2000). The ATPase cycle of Hsp90 drives a molecular "clamp" via transient dimerization of the N-terminal domains. EMBO J. *19*, 4383–4392.

Roe, S.M., Prodromou, C., O'Brien, R., Ladbury, J.E., Piper, P.W., and Pearl, L.H. (1999). The structural basis for inhibition of the Hsp90 molecular chaperone, by the anti-tumour antibiotics radicicol and geldanamycin. J. Med. Chem. *42*, 260–266.

Roussel, A., and Cambillau, C. (1991). TURBO. In Silicon Graphis Geometry Partners Directory (Mountain View, CA: Silicon Graphics Inc.), pp. 77–78.

Sato, S., Fujita, N., and Tsuruo, T. (2000). Modulation of akt kinase activity by binding to hsp90. Proc. Natl. Acad. Sci. USA *97*, 10832–10837.

Scheibel, T., Weikl, T., and Buchner, J. (1998). Two chaperone sites in Hsp90 differing in substrate specificity and ATP dependence. Proc. Natl. Acad. Sci. USA *95*, 1495–1499.

Schulte, T.W., Blagosklonny, M.V., Ingui, C., and Neckers, L. (1995). Disruption of the Raf-1-Hsp90 molecular complex results in destabilization of Raf-1 and loss of Raf-1-Ras association. J. Biol. Chem. *270*, 24585–24588.

Setalo, G., Singh, M., Guan, X.P., and Toran-Allerand, C.D. (2002). Estradiol-induced phosphorylation of ERK1/2 in explants of the mouse cerebral cortex: the roles of heat shock protein 90 (Hsp90) and MEK2. J. Neurobiol. *50*, 1–12.

Silverstein, A.M., Grammatikakis, N., Cochran, B.H., Chinkers, M., and Pratt, W.B. (1998). P50(cdc37) binds directly to the catalytic domain of Raf as well as to a site on hsp90 that is topologically adjacent to the tetratricopeptide repeat binding site. J. Biol. Chem. *273*, 20090–20095.

Stancato, L.F., Chow, Y.-H., Hutchinson, K.A., Perdew, G.H., Jove, R., and Pratt, W.B. (1993). Raf exists in a native heterocomplex with

Hsp90 and p50 that can be reconstituted in a cell-free system. J. Biol. Chem. *268*, 21711–21716.

Stebbins, C.E., Russo, A.A., Schneider, C., Rosen, N., Hartl, F.U., and Pavletich, N.P. (1997). Crystal structure of an Hsp90-geldanamycin complex: targeting of a protein chaperone by an antitumor agent. Cell *89*, 239–250.

Terwilliger, T.C. (2000). Maximum likelihood density modification. Acta Crystallogr. D *56*, 965–972.

Terwilliger, T.C., and Berendzen, J. (1999). Automated structure solution for MIR and MAD. Acta Crystallogr. D *55*, 849–861.

Tingey, A.P., and Maxwell, A. (1996). Probing the role of the ATP-operated clamp in the strand-passage reaction of DNA gyrase. Nucleic Acids Res. *24*, 4868–4873.

Whitesell, L., Mimnaugh, E.G., De Costa, B., Myers, C.E., and Neckers, L.M. (1994). Inhibition of heat shock protein HSP90-pp60v-src heteroprotein complex formation by benzoquinone ansamycins: essential role for stress proteins in oncogenic transformation. Proc. Natl. Acad. Sci. USA *91*, 8324–8328.

Wigley, D.B., Davies, G.J., Dodson, E.J., Maxwell, A., and Dodson, G. (1991). Crystal structure of an N-terminal fragment of the DNA gyrase B protein. Nature *351*, 624–629.

Wimberly, B.T., Brodersen, D.E., Clemons, W.M., Morgan-Warren, R.J., Carter, A.P., Vonrhein, C., Hartsch, T., and Ramakrishnan, V. (2000). Structure of the 30S ribosomal subunit. Nature *407*, 327–339.

Xu, Y., Singer, M.A., and Lindquist, S. (1999). Maturation of the tyrosine kinase c-Src as a kinase and as a substrate depends on the molecular chaperone Hsp90. Proc. Natl. Acad. Sci. USA *96*, 109–114.

Young, J.C., Schneider, C., and Hartl, F.U. (1997). In vitro evidence that hsp90 contains two independent chaperone sites. FEBS Lett. *418*, 139–143.

Accession Numbers

Coordinates and structure factors have been deposited in the Protein Databank with PDB code 1HK7.